

UDC 662.612, 004.932

*A. Kotyra, W. Wójcik, K. Gromaszek*  
Lublin University of Technology, Poland  
38a, Nadbystrzycka str., Lublin, 20-618

## DETERMINATION OF BIOMASS CO-COMBUSTION PROCESS STATE BASED ON FLAME IMAGE SERIES ANALYSIS

*A. Котюра, В. Вуйцик, К. Громашек*  
Люблінський технологічний університет, Польща  
вул. Надбистшицька, 38а, м. Люблін, 20-618

## ВИЗНАЧЕННЯ СТАНУ ПРОЦЕСУ СПІЛЬНОГО СПАЛЮВАННЯ БІОМАСИ НА ОСНОВІ АНАЛІЗУ ПОСЛІДОВНОСТІ ЗОБРАЖЕНЬ ПОЛУМ'Я

The article presents an approach to use some base frequency parameters of flickering such as the frequency having the largest amplitude (base frequency) and centroid of amplitude spectrum for characterization of different combustion process state. The laboratory test stands enabled scaled down 10:1 combustion conditions. Analysis results show that the frequency spatial information could be helpful in combustion process diagnostics.

**Keywords:** biomass co-combustion, image processing, flame flicker.

У статті запропоновано підхід до використання параметрів базової частоти мерехтіння, таких як базова частота та центроїд амплітудного спектра для характеристики різних станів процесів згорання. Стенд лабораторного випробування дозволив знизити умови горіння 10:1. Результати аналізу показують, що просторова інформація частоти може бути корисною для діагностики процесу згорання.

**Ключові слова:** спалювання біомаси, обробка зображень, полум'яний флікер.

### Introduction

Climate protection becomes more and more severe problem. Renewable fuels are considered as one of the main ways of reducing greenhouse-gas emissions, primarily CO<sub>2</sub> for it is absorbed during plant growth and released during combustion. Hence, it does not contribute to the greenhouse effect.

The most common and cheapest method of energetic biomass utilization is its direct firing or co-firing with other solid fuels, particularly with coal in the existing power plants. Another means of its exploitation, mainly in thermo-chemical conversion technologies such as pyrolysis, gasification, anaerobic digestion has minor significance in bio-energy production [1].

Biomass is a highly volatile fuel. The rate of pulverised biomass combustion is considerably higher than that of coals [1] being more similar to oil or gas fuels combustion [1, 2]. However, biomass-coal co-firing has several significant drawbacks. Biomass contains less carbon and more oxygen than coal, that results in a lower heating value. High moisture, as well as ash content, can be a reason of possible combustion stability problem. On the other side, higher chlorine contents rise corrosion rate. The melting point of the ash can be low. It causes increased slagging and fouling of combustor surfaces that reduce heat transfer and result in corrosion and erosion problems [3]. Biomass has lower density and friability than coal that results in possible stratification of fuel mixture contents during its conveyance to burners. What is more, both physical and chemical biomass parameters of biomass are unsteady in time [4]. All the mentioned factors make the co-combustion process difficult to maintain. Thus, ensuring the proper operating point of the combustion process requires diagnostic system, that would enable to discriminate combustion process

states, especially the ones when the process runs in a wrong way leading to raised emissions of harmful substances, malfunctions or even threat to human life.

Majority of the systems intended to keep the combustion process within the permissible boundaries utilize analysis of flue gases. The information retrieved is delayed and averaged among many burners operating inside a typical combustion chamber in power plant. Furthermore, it is hard to determine which burner operates improperly for the information obtained is not spatial.

An approach that is based on flame radiation analysis has no drawbacks mentioned above. Combustion of pulverized fuels takes place in a turbulent flow. Local fluctuations occur of both fuel and gaseous reagents concentrations, as well as temperature. It leads to permanent local changes in the combustion process intensity that results in continuous changes in flame luminosity which can be observed as flame flicker. Combustion process affects the turbulent movement of its products and reagents determine the way the flame flicker parameters such as e.g. mean luminosity. For a given fuel mixture at constant air and fuel flow, the combustion process remains in statistical equilibrium. Thus, flame flicker is a pointer of ongoing combustion process that is commonly applied in flameout protection systems. However, such systems evaluate from having single optical channel to multi-channel and even image processing based [5, 6, 7, 8].

The article presents an approach to use some base frequency parameters of flickering such as the frequency having the largest amplitude (base frequency) and centroid of amplitude spectrum for characterization of different combustion process state.

#### Laboratory combustion tests

Combustion tests were done in a 0.5 MW<sub>th</sub> (megawatt of thermal) research facility, enabling scaled down (10:1) combustion conditions. The main part is a cylindrical combustion chamber of 0.7 m in diameter and 2.5 m long. A low-NO<sub>x</sub> swirl burner about 0.1 m in diameter is mounted horizontally at the front wall. The stand is equipped with all the necessary supply systems: primary and secondary air, coal, and oil. Pulverized coal for combustion is prepared in advance and dumped into the coal feeder bunker. Biomass in a form of straw is mixed (10% by mass) with coal after passing through the feeder.

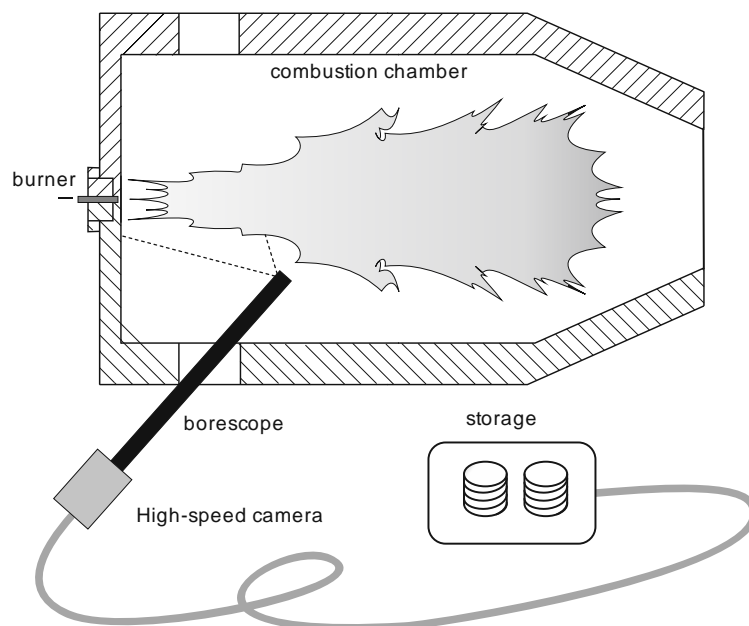


Fig. 1. Laboratory setup

The combustion chamber has two lateral inspection openings on its both sides, that provide optical access. A borescope with high-speed camera attached was placed near burner's nozzle, as shown in fig. 1. The camera has a color CMOS area scan sensor capable to catch 500 frames per second (fps). The borescope's direction of view was 90 degrees to its axis. Flame images were transferred from the interior of the combustion chamber through a 0.7m borescope and were captured at a speed of 150 fps at full resolution ( $1280 \times 1024$  pixels), transferred and then stored in a high-performance storage system. The optical parts were cooled with water jacket. Additionally, purging air was used to avoid dustiness.

Several combustion tests were performed during which blend of pulverized coal and straw was burned for different settings of the combustion facility. Fuel and air flow rates were set independently and kept at the same level. The scale measured amount of fuel that was stored in the bunker. As the feeder had delivered the fuel blend to the burner, scale readings had tended to decrease. Fuel flow was calculated as a quotient of difference between two successive readings of scale and length of time interval between them. The experiment took about four hours while image sequence recordings lasted for about 30 seconds during which combustion state was in stationary condition. It was due to vast amount of storage memory that would be needed during the whole combustion test that usually lasted for 3 up to 5 hours. The fuel and air flows, as well as the other parameters of the stand were recorded in one second intervals whereas several images captured is equal to 150.

Nine combustion states were set. During the first three, fuel flow was comparatively high, reaching 58–68 kg/h whereas fuel flow was adjusted at three levels. The fourth recording was made at the lowest fuel flows (around 20kg/h) with higher, but not steady air flow. The next two combustion process states fuel flow rate was around 50kg/h with higher and lower air flows, respectively. The last three states were conducted at fuel flows rate slightly lower than 40 kg/h.

Color images (24bit RGB) of flame were captured for mentioned above variants and stored in an uncompressed form. Example two sequences for two different combustion states were presented in figure 2. As it can be noticed, flame shape is different for different settings of air as well as pulverized fuel flow rate.

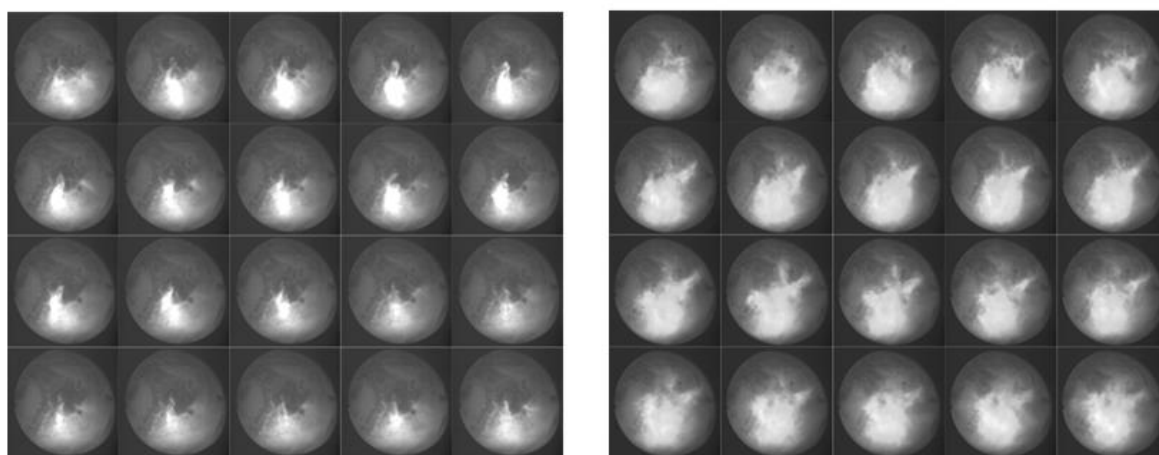


Fig. 2. An example frame sequences captured for two different settings of fuel and air flows

### The methods

A sequence of  $N$  images was compacted in a single 3-dimensional data structure. The two spatial dimensions ( $x, y$ ) corresponded to coordinates of each pixel of a single frame, whereas the third dimension – to a time at which the given frame was captured. The image sequence consisted of time series matched to each frame pixel of known coordinates as shown in figure 3.

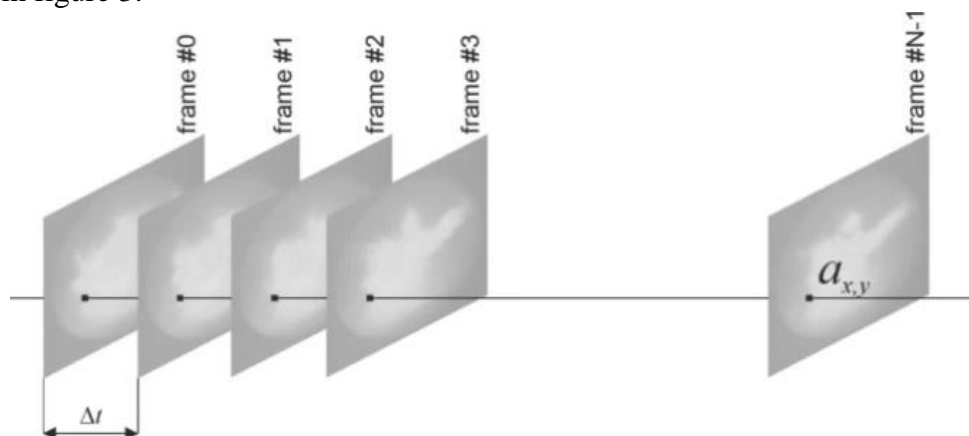


Fig. 3. Data structure containing image sequence

An example time series that was obtained for a given pixel coordinate  $x, y$  is presented in Figure 3. Since the images were processed as 8-bit greyscale, the pixel amplitude was between 0 and 255. Before performing the frequency analysis of the data obtained, the mean value was subtracted. Time series for each coordinate ( $x, y$ ) in image sequence were analysed in frequency domain in order to determine spatial distribution of flame flicker. For that case, amplitude spectrum ( $A_{x,y}$ ) can be expressed in the form of the following equation:

$$A_{x,y}(f_q) = \left| \sum_{k=0}^{N-1} a_{x,y}(t_k) \exp(-j2\pi f_q t_k) \right|, \quad (1)$$

where  $f_q$  – discrete frequency  $q^{\text{th}}$  sample ( $q = 0, 1, 2 \dots N-1$ ).

The number of images that are captured in one second (fps) is  $1/\Delta t$  where  $\Delta t$  denotes time resolution (distance between two neighbouring time samples). The maximum frequency of flame flickering that can be determined  $f_{\text{max}}$  can be calculated based on the Shannon-Kotelnikov theorem:

$$f_{\text{max}} = \frac{1}{2\Delta t} = \frac{\text{fps}}{2}. \quad (2)$$

As the number of samples in time and frequency domains equal  $N$ , the frequency resolution  $\Delta f$  can be expressed as:

$$\Delta f = \frac{\text{fps}}{N}. \quad (3)$$

The spectra obtained were characterized by the frequency of highest magnitude and spectral centroid that is defined as [9]:

$$\text{centroid}_{x,y} = \frac{\sum_{k=0}^{N-1} |A_{x,y}(f_k)| f(t_k)}{\sum_{k=0}^{N-1} |A_{x,y}(f_k)|} \quad (4)$$

During the data acquisition, the combustion process remained in stationary conditions. The single image series recording lasted 40 seconds at a rate of 150fps, that corresponded to  $N = 6000$  points in time domain. The resolution of each captured image was  $800 \times 800$  pixels yielding a total number of 64000 time series. According to Nyquist Sampling Theorem, the maximum resolvable frequency is 75Hz and following eq. (4) the frequency resolution obtained was 0.025Hz. The amplitude spectrum obtained for an example time series is presented in figure 4.

As it can be observed in the spectrum plot, majority of flame flicker power is contained within frequencies of about 1Hz. Thus, it is necessary to provide the frequency resolution at least of the order of 0.1Hz.

The laboratory tests were conducted for several combustion states with different settings of fuel and secondary air flows and different biomass content 10% and 30%. The air flow was determined by stoichiometry and amount of fuel delivered in a unit of time for a constant excess air coefficient ( $\lambda$ ) that is defined as a quotient the mass of air to combust 1kg of fuel to mass of stoichiometric air. For that reason, secondary air flows for the same  $\lambda$  are different for different settings of fuel flow.

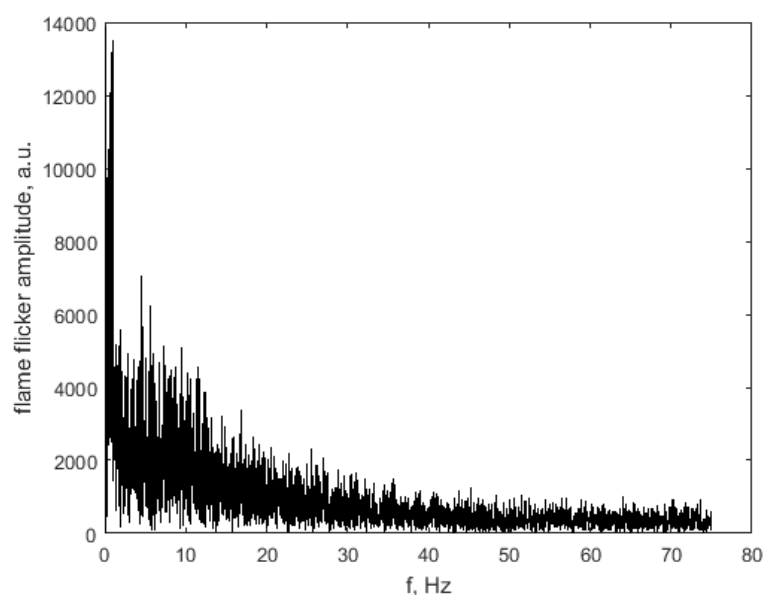


Fig. 4. Amplitude spectrum obtained for an example time series

## Results

Each combustion state was determined by thermal load and the corresponding excess air coefficient. The desired value of thermal load was adjusted by a proper fuel flow of known calorific value. Results of centroid distribution for flame flicker for selected combustion tests are presented in fig. 5. It can be noticed the distribution is almost uniform regardless of thermal load of the combustion test stand  $\lambda$ , and biomass content in mixture. The centroid frequency is approximately 0.5Hz.

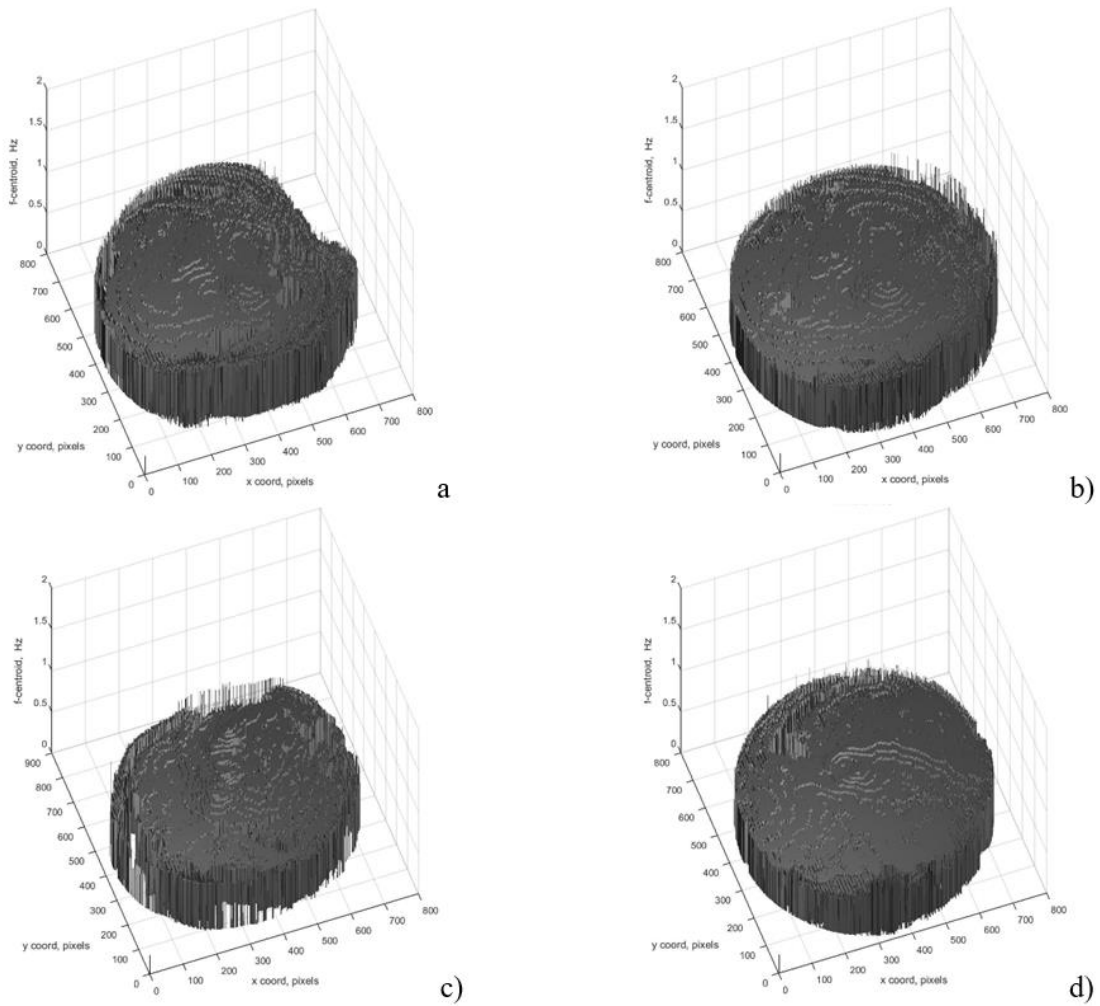


Fig. 5. Spatial distribution of flame flicker frequency centroid for: 10% of biomass in mixture,  $\lambda = 0.75$ ,  $P_{th} = 250\text{kW}$  – a);  $P_{th} = 380\text{kW}$  – b); 30% of biomass in mixture,  $\lambda = 0.75$ ,  $P_{th} = 250\text{kW}$  – c),  $P_{th} = 380\text{kW}$  – d)

Figure 6 presents spatial distributions of amplitude corresponding to each centroid presented in figure 5. It can be noticed, distribution of frequency with maximal amplitude is different for each combustion state. Slightly higher frequencies can be spotted in the very centre, where burner is located, reaching about 1.0 – 2.5 Hz. Lower frequencies (nearly 0Hz) correspond to the region where the radiation emitted by the flame was reflected by inner parts of the combustion chamber.

### Conclusions

Due to borescope placement constraints, the burner is located in the middle of the captured images and the near-burner zone, cannot be observed from side view. This is undesired place of probe mounting, however in industry conditions, it is sometimes hard to gain optical access in a better place in the combustion chamber. The spotted flame flicker frequencies of the highest amplitudes, as it was mentioned before, are around 1Hz. As it can be observed in figure 4, amplitudes of flame flicker frequency drop exponentially, remaining on the same level above 40–45Hz.

The length of time window was appropriate to determine frequencies with the resolution of 0.025Hz. The analysis presented has revealed that centroid of the flame flicker amplitude spectrum cannot enable discrimination of different combustion process states.

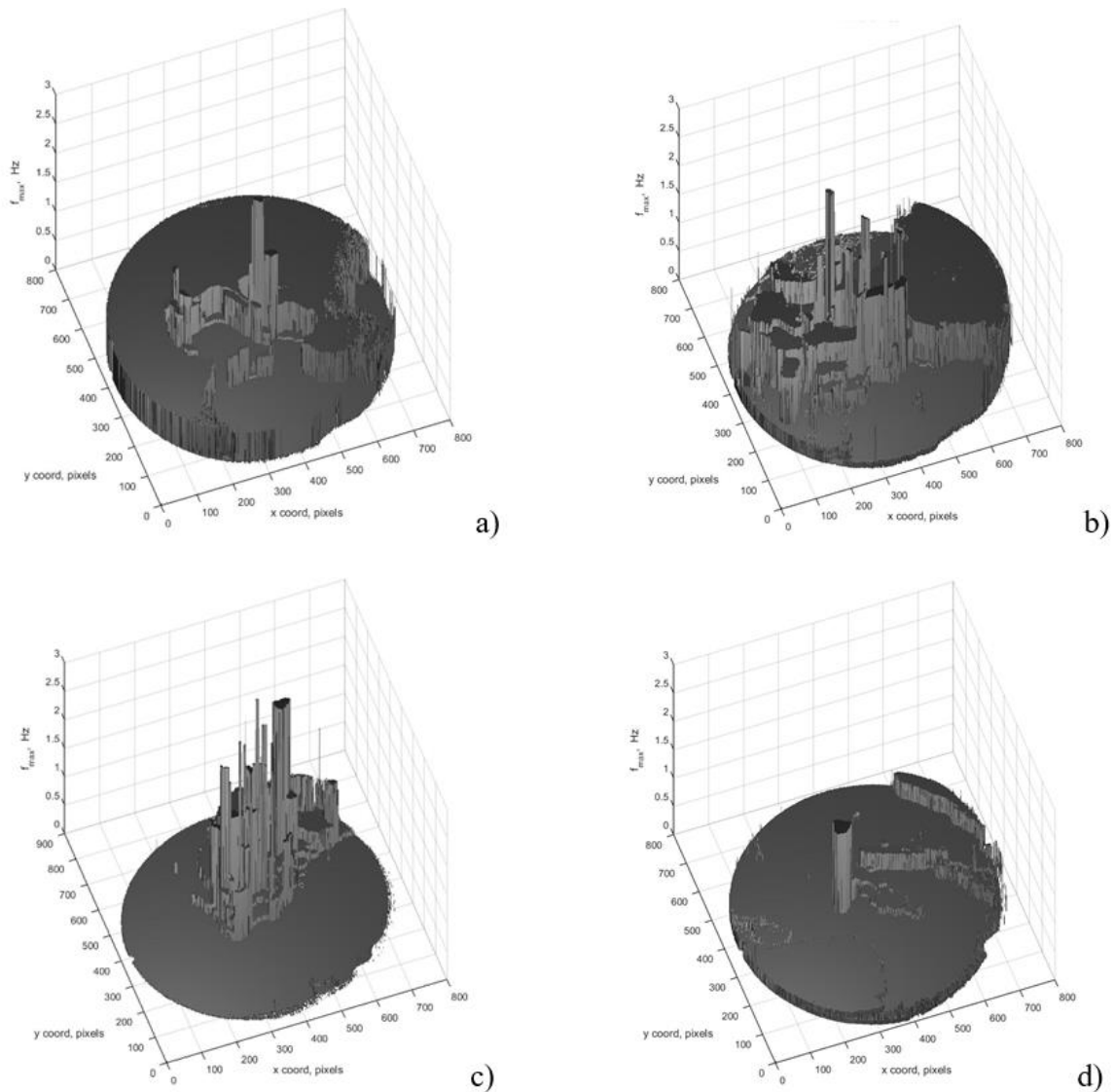


Fig. 6. Spatial distribution of the frequency having the maximum amplitude for: 10% of biomass in mixture,  $\lambda = 0.75$ ,  $P_{th} = 250\text{kW}$  – a);  $P_{th} = 380\text{kW}$  – b); 30% of biomass in mixture,  $\lambda = 0.75$ ,  $P_{th} = 250\text{kW}$  – c),  $P_{th} = 380\text{kW}$  – d)

Different situation takes place for the case of the second parameter being examined, i.e. spatial distribution of flame flicker frequency having the maximal amplitude. The results obtained have pointed, it is discriminative parameter. The highest frequencies can be found in the very centre of the examined frames, where burner outlet is present and velocities of air fuel mixture have higher values. The frequency distributions are different both regarding fuel flow (fig. 6a, 6b and fig. 6c, 6d) and biomass content in fuel mixture. Higher biomass content (30% - fig 6c, 6d) corresponds to almost zero frequency outside the burner.

The frequency spatial information could be helpful in combustion process diagnostics. Comparing to pure amplitude information as irradiance, it is more immune to

presence of dust that affects operation of optical parts inside a combustion chamber. The frequency profiles presented are specific for a given burner type, fuel and combustion chamber and for every case should be determined independently.

### References

1. Demirbas A. Recent advances in biomass conversion technologies, Energy Edu Sci Technol., No 6, 2000. P. 19-41.
2. Marks J. Wood powder: an upgraded wood fuels: the role of renewables, Forest Products Journal, No 42, 1992. P. 52-58.
3. Pronobis M. The influence of biomass co-combustion on boiler fouling and efficiency. Fuel 85, 2006. P. 474-480.
4. Sami M., Annamalai K., Wooldridge M. Co-firing of coal and biomass fuel blends, Progress in Energy and Combustion Science, 27, 2001. P. 171-214.
5. Ballester J., García-Armingol T. Diagnostic techniques for the monitoring and control of practical flames, Prog Energy Combust. 36, 2010. P. 375-411.
6. Docquier N., Candel S. Combustion control and sensors: a review. Prog Energy Comb Sci 28, 2002. P. 107-50.
7. Demirbas A. Combustion characteristics of different biomass fuels. Progress in Energy and Combustion Science 30, 2004. P. 219-230.
8. Lu G., Gilbert G., Yan Y. Vision based monitoring and characterization of combustion flames. Journal of Physics: Conference Series 15, 2009. P. 194-200.
9. Kua J.M.K., Thiruvanan T., Nosratighods M., Ambikairajah E., Epps J. Investigation of spectral centroid magnitude and frequency for speaker recognition. In Proc. Odyssey, The Speaker and Language Recognition Workshop, Brno, Czech Republic, 2010. P. 34-39.

### РЕЗЮМЕ

*A. Kotyra, W. Wójcik, K. Gromaszek*

**Визначення стану процесу спільного спалювання біомаси на основі аналізу послідовності зображень полум'я**

У статті представлений підхід до використання інформації, що міститься у випромінюванні полум'я для виявлення процесу спалювання біомаси. Підхід полягає в обробці послідовностей зображень, отриманих з камери згоряння, та проведення частотного аналізу часових рядів, що відповідають кожному пікселю зображення. Параметри базової частоти досліджувались як частота, що має найбільшу амплітуду (базову частоту) і центроїд амплітудного спектра. Дані були зібрані під час декількох випробувань спільного спалювання біомаси, які виконувалися для різних параметрів горіння - теплових навантажень (250 кВт та 380 кВт) та кількості біомаси в суміші (10%, 30%). Лабораторний тестовий стенд (макс. 500кВт) дозволив зменшити (10:1) умови згоряння. Зображення були отримані за допомогою високошвидкісної CMOS-камери з приєднаним до водяного охолодження борескопом, об'єднаних з високопродуктивною системою зйомки зображень. Результати аналізу були представлені у вигляді просторових розподілів зазначених частотних параметрів. Обговорення результатів в основному зосереджене на можливостях застосування у діагностичних цілях при визначенні стану процесу згоряння.

*Надійшла до редакції 21.09.2017*